Measurements of shear wave velocity by resonant-column test, bender element test and miniature accelerometers

Javier Camacho-Tauta
Nueva Granada Military University, Bogotá, Colombia
Giovanni Cascante
University of Waterloo, Waterloo, Canada
Jaime A. Santos
Technical University of Lisbon, Lisbon, Portugal
António Viana da Fonseca
University of Porto, Porto, Portugal

ABSTRACT
Bender elements (BE) have been widely utilized to measure shear wave velocities at low shear strain. One of the most controversial issues is the lack of knowledge of the actual behaviour of the BE inside the soil. BE tests were compared with resonant-column tests and readings of miniature accelerometers inside the specimen at different elevations. While time domain (TD) analysis produced reasonable results, frequency domain (FD) analysis showed significant differences. Experimental measurements and simplified numerical simulations revealed the existence of several peaks in the transfer function between BE. These peaks produce slight variations in the slope of the phase angle function, affecting the travel time estimation. FD analysis should be done in a frequency range located far away to the main peaks, requiring a careful selection of the input signal depending of the soil stiffness, characteristics of BE and specimen dimensions.

PRESENTACIONES TÉCNICAS
El ensayo de Bender elements (BE) ha sido ampliamente utilizado para medir la velocidad de la onda cortante a baja deformación. Uno de los aspectos mas controvertidos es el poco conocimiento acerca del comportamiento de estos elementos dentro del espécimen. Se compararon ensayos BE con ensayos de columna resonante y lecturas de acelerómetros miniatura localizados a diferentes elevaciones. Mientras los análisis en el dominio del tiempo (TD) concordaron razonablemente, los análisis en el dominio de la frecuencia (FD) mostraron diferencias significativas. Resultados experimentales y simulaciones numéricas simplificadas mostraron múltiples picos en la función de transferencia entre el par de BE. Estos picos coinciden con ligeras variaciones en la pendiente del ángulo de fase, afectando la estimación del tiempo de viaje. El análisis FD debería realizarse en un rango frecuencial alejado de los picos principales, requeriendo una cuidadosa selección de la señal de entrada, dependiendo de la rigidez del suelo, las características de los BE y las dimensiones del espécimen.

1 INTRODUCTION

Bender elements (BE) have been widely utilized to measure shear wave velocities at low shear strain levels ($\gamma<10^{-6}$). The simple operation of these transducers has stimulated their use in a variety of geotechnical equipment since their first appearance (Shirley, 1978; Shirley and Hampton, 1978). A voltage signal is applied to a piezoceramic element (transmitter), which generates a small shearing perturbation that travels from one end of the specimen to the opposite side; similarly, a piezoceramic element (receiver) transforms a mechanical perturbation in an output voltage. The time difference between the emitted and received signals and the distance between transducers are used to compute the shear wave velocity of the material (Dyvik and Madshus, 1985). Many researchers have studied different issues on the application of bender elements for geotechnical characterization. However, BE testing is not yet a standard because of the variability of the results in comparison to the standard resonant-column test (ASTM International, 2002).

The wave propagation in BE tests have been widely studied theoretically and experimentally. The reliability of BE testing is influenced by different factors such as near-field effects (Sanchez-Salinero *et al.*, 1986; Brignoli *et al.*, 1996; Arulnathan *et al.*, 1998; Arroyo *et al.*, 2003; Lee and Santamarina, 2005); directivity (Lee and Santamarina, 2005); travel distance (Brignoli *et al.*, 1996); boundary effects (Arulnathan *et al.*, 1998); sample geometry and size (Rio *et al.*, 2003; Arroyo *et al.*, 2006) and crosstalk (Lee and Santamarina, 2005).

At first, square waves were used as excitation voltage because of their simplicity and high impulse energy. However, Viggiani and Atkinson (1995) recommended the use of a single sinusoidal input pulse; because, this signal has a narrower frequency spectrum; and the output signal is expected to have a similar shape. The sinusoidal pulse is currently used in many laboratories (Yamashita *et al.*, 2009). Arulnathan *et al.* (1998) analyzed different methods for the interpretation of BE tests; which include the evaluation of the travel time using characteristic peaks of input and output signals, the cross-correlation of input and output signals, and phase analysis of the cross-power

spectrum. They also used the time lag between the first and second arrival in the output signal. Given the variability in the results, the use various methods is recommended (Jovičić *et al.*, 1996).

Greening and Nash (2004), based on the phase delay method (Kaarsberg, 1975) developed a methodology in which the evaluation of the travel time is made in the frequency domain. They used a broadband sinusoidal sweep as excitation signal. The travel time is computed from the slope of the unwrapped phase angle of the cross-power spectrum. An analysis framework that combines time-domain and frequency-domain methods was proposed by Viana da Fonseca *et al.* (2009). First, sine-wave pulses at different frequencies are used to evaluate the first arrival. Then, sinusoidal sweeps are applied and the results analyzed for different frequency ranges (Santos *et al.*, 2007; Camacho-Tauta *et al.*, 2008).

One of the most important issues in BE testing is the lack of knowledge of the actual behaviour of the piezoceramic elements inside the soil specimen (Lee and Santamarina, 2005). Pallara *et al.*(2008)compared the input signal used to excite the bender transmitter and its actual movement measured by a laser diode, showing that the last is delayed and asymmetric with respect to the original signal. Rio (2006) measured the BE response to sinusoidal pulses and sine sweep excitations using a laser Doppler Velocimeter (LDV) under free and embedded conditions. Under free conditions, the response of the transmitter is dominated by its own resonant frequency rather than the excitation frequency. Whereas for embedded conditions, the natural frequency increases due the stiffening of the medium, the damping ratio increases and the magnitude of the oscillation decreases.

Previous researchers used miniature accelerometers to measure shear wave velocities (Nishio and Tamaoki, 1988; Maqbol and Koseki, 2008; Wicaksono *et al.*, 2008).They located accelerometers in the external boundary of the specimen and used sources of excitation different than BE. Recently, Ferreira *et al.* (2010) shows an arrangement of BE and external accelerometers.

The purpose this paper is to obtain experimental evidence of the actual performance of a BE system in dry sand specimens. The response of the BE system is compared with resonant-column tests and with the response of miniature accelerometers inside the specimen at different elevations. BE and accelerometer data are analyzed in the time domain and also in the frequency domain. Experimental results and simplified numerical simulations allow identifying the main causes of the discrepancies of the frequency domain method. Suggestions are done in order to minimize such causes.

2 INTERPRETATION AND ANALYSIS OF BE TESTS

The principle of BE testing is simple; however, a clear identification of the arrival time is not always possible; and different interpretation methods have been proposed. Currently, there is not a single and accurate technique that can be adopted as standard. Methods of test and analysis can be classified into two categories: time domain (TD) and frequency domain (FD).

2.1 TD analysis

TD analysis used in this paper is based on the detection of the first arrival in the received signal when the input excitation is a single sine pulse.

2.2 FD analysis

Kaarsberg (1975) observed that using a continuous sine signal at frequency f, the wave velocity is given by

$$V_s=\lambda \cdot f \qquad [1]$$

The wavelength λ is not measured directly but using the phase lag between input and output signals. The group wave velocity V_{gr} is given as the derivative of the frequency with respect to the wave number k, by

$$V_{gr}=2\pi\frac{df}{dk} \qquad [2]$$

The wave number can be expressed in terms of the phase lag ϕ, between input and output signals and the distance between BE L_{tt},($k = \phi/L_{tt}$). Eq. 2 can be expressed as:

$$V_{gr}=2\pi\frac{df}{d\phi}L_{tt} \qquad [3]$$

Hence, the travel time t_t is (Greening and Nash, 2004):

$$t_t=\frac{1}{2\pi}\frac{d\phi}{df} \qquad [4]$$

Thus, the travel time is estimated from the slope of the phase function obtained from the transfer function between the two signals. Greening and Nash (2004) pointed out that a sine sweep excitation is a logical progression of the method proposed by Kaarsberg (1975).

FD analysis requires transformation of the time signals using Fourier transformations: the transfer function H(f) between transmitter T(t) and receiver R(t) is given in terms of the average cross power spectral density $\overline{G_{RT}}$ and the average auto spectral density $\overline{G_{TT}}$ as

$$H(f)=\frac{\overline{G_{RT}}}{\overline{G_{TT}}} \qquad [5]$$

The average of spectral densities is used to reduce the effect of noise. The linearity of the transfer function is measured by the coherence function γ^2 given by

$$\gamma^2(f)=\frac{|\overline{G_{RT}}|^2}{\overline{G_{TT}}\cdot\overline{G_{RR}}} \qquad [6]$$

The slope of the unwrapped phase function is computed using linear regression procedures. Then, the travel time is calculated by Eq.4.In general, the unwrapped phase angle function does not have perfectly constant slope even for coherence close to unity. Hence, Ferreira *et al.* (2006) and Viana da Fonseca *et al.* (2009) estimated the travel time by plotting the travel time computed from various frequency bandwidths as a function of the frequency and selecting the most probable value taking into account the coherence and the frequency band where the travel time is more stable.

2.3 Resonant frequency of BE in soil

Lee and Santamarina (2005) derived Eq. 7 for the first resonant frequency (f_r) of the equivalent BE-soil system by taking into account the BE and soil stiffness, k_b and k_s, and the BE and soil mass, m_b and m_s.

$$f_r=\frac{1}{2\pi}\sqrt{\frac{k_b+k_s}{m_b+m_s}} \qquad [7]$$

with

$$k_b=1.875^4\,\frac{E\cdot I}{(\alpha L)^3} \quad k_s=2\eta V_S^2\rho_s(1+v)L \qquad [8]$$

$$m_b=\alpha\rho bhL \qquad m_s=\rho_s b^2 L\beta$$

Where the soil properties are: V_S is the shear wave velocity, ρ_s is the soil mass density, and v is the Poisson's ratio.

The properties of the BE are: E is the Young's modulus, ρ is the mass density, L is the length, b is the width, h is the thickness, and I is the area moment of inertia ($I=bh^3/12$).

Other factors are: α is the effective length factor (α=1 for perfectly fix conditions at the base; α>1 for flexible base conditions), β is an experimental factor related with the volume of soil mass affecting the vibration of BE and η is the mean displacement influence factor at the soil-element interface (η≈2).

Experimental resonant frequencies for different confinements (i.e. different stiffness) can be used to obtain α and β for a particular BE-soil system.

3 EXPERIMENTAL SETUP

A Stokoe-type resonant-column (RC) device (Cascante *et al.*, 2005) is equipped with a set of bender elements (Ismail *et al.*, 2005) and miniature accelerometers (Dytran, Model 3035B). This new configuration is used to perform RC tests and BE tests while simultaneously recording particle accelerations inside the specimen at different heights. The cell pressure is controlled by a pneumatic system with a maximum confinement of σ_0 =700 kPa. The specimens are in average 14 cm in height and 7 cm in diameter. Figure 1 shows a schematic of the system.

The Resonant-Column system is composed of a dynamic signal analyzer (HP-35670A); which generates a signal that is amplified by a power amplifier (Bogen, GS-250).

The amplified signal drives the four pairs of coils; which induce a magnetic field on the set of magnets that produces a torsional excitation to the specimen. The response of the system is measured by an accelerometer (PCB352A78) attached to the driving plate. The accelerometer is fed by a power source unit (Dytran 4121). Both signals in the coils and the accelerometer are filtered and amplified by a signal conditioning system (Krohn-Hite 3384) and monitored by a digital oscilloscope. The Fourier spectra are computed in real time by the dynamic signal analyzer.

The transmitter BE is located at the base pedestal of the resonant-column device; which is excited by an arbitrary wave generator (Physical Acoustics Corp). The receiver BE is located at the top cap; its output signal is conditioned using a filter-amplifier (Krohn-Hite 3384).

Miniature accelerometers (Dytran3035B) are placed at various locations inside the sand specimen. The accelerometers are placed during the specimen preparation by the dry compaction method. The thin and flexible wire of the accelerometer passes through the membrane by a small hole that is sealed with silicone. The accelerometers are powered and amplified by a power source (Dytran 4123B). The input and output signals are collected by a data acquisition system (LDS-Nicolet, Genesis IDH362, 1MS/s per channel).

4 EXPERIMENTAL METHODOLOGY

A specimen of Toyoura sand was prepared by the dry pluviation method (Diameter = 70mm, length = 138.3mm, total dry mass = 810.22g, void ratio, e = 0.732). Four accelerometers were placed inside the specimen according to the drawing shown in Figure 2. Acc. 3 failed and their recordings were not consistent. For this reason, these readings were not used for analysis. The specimen was subjected to four different confinement pressures, σ_0: 50, 100, 200 and 400 kPa. In each stage, TD and FD tests were carried out with simultaneous measurements of accelerations. After these tests, RC tests were performed.

4.1 TD tests

The frequency of the single pulse used in TD tests was selected as the frequency that produced the highest response by the receiver and at the same time it should guarantee $L_{tt}/\lambda>2$ in order to reduce the near-field effect (Arroyo *et al.*, 2003).

Figure 3 shows an example of the time charts obtained in the TD tests. Signals are represented in normalized amplitude and the maximum amplitude of each of them is indicated in the caption (in volts or gravity units, according to the type of sensor). The secondary vertical axis at the right side of the figure represents the elevation of each sensor. The inclined line joins the estimated arrival times of each sensor. The slope of this line is the average shear wave velocity.

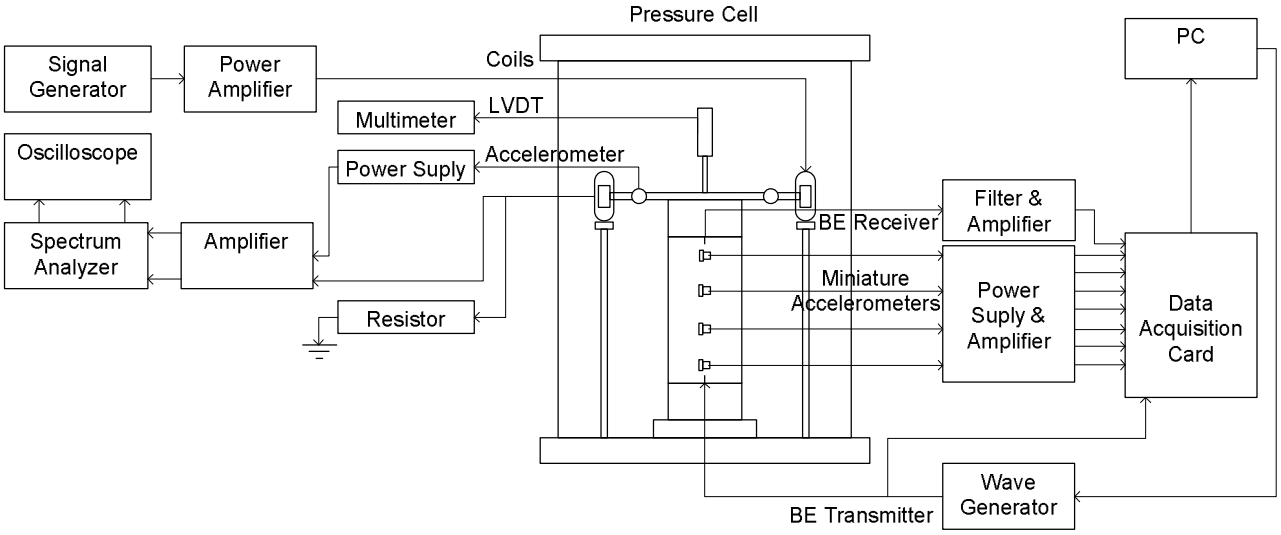

Figure 1.Schematic description of the resonant-column device with bender elements and miniature accelerometers

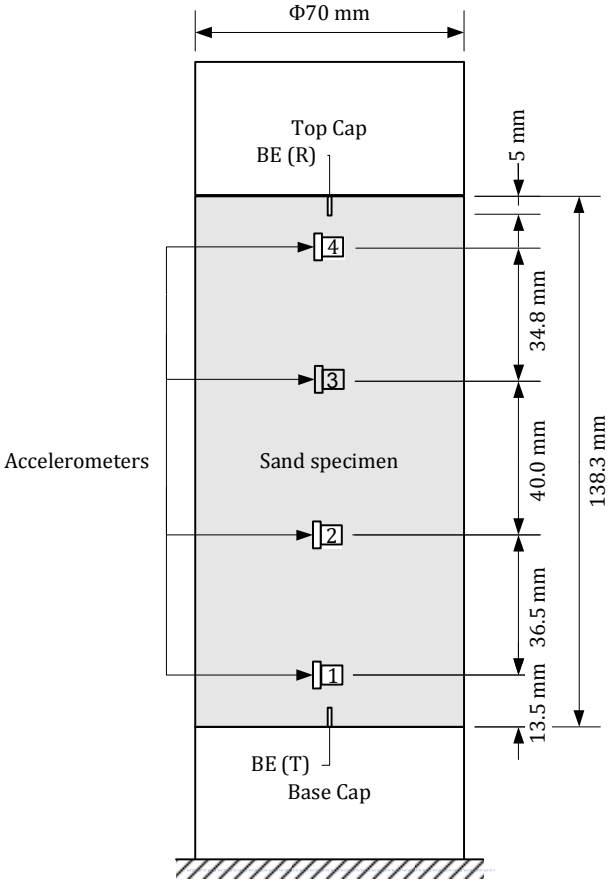

Figure 2. Drawing of the specimen of Toyoura sand showing location of BE and internal accelerometers

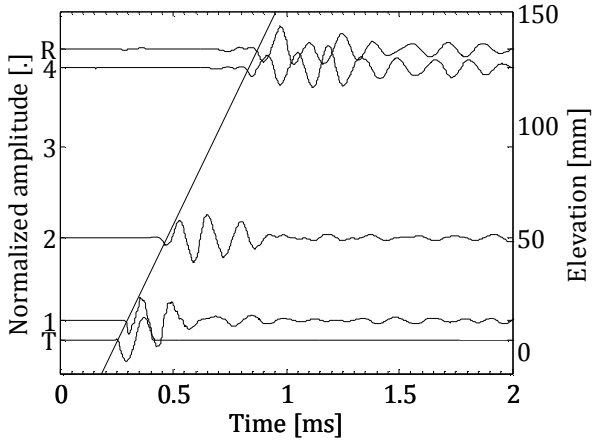

Figure 3. TD test (σ_0=50 kPa) Maximum amplitude: T[9.943V]; 1[0.620g]; 2[0.392g]; 4[0.382g]; R[0.016V]

4.2 FD tests

The characteristics of the sine sweep signal were: 10 V amplitude, 12ms period and frequency content between 1 to 20 kHz. Figure 4 shows an example of the time signals recorded in the FD test. The amplitude is represented in normalized scale. The total record is 15 ms long to provide information before the trigger and after the signals decay. There is a gradual change in the shape of the signal, as the sensor is further away from the transmitter.

FD tests are better represented in the frequency domain, as shown in Figure 5. The normalized power spectra exhibit some common peak frequencies identified by a vertical line. Such frequencies are present in all sensors. Other frequencies attenuate gradually with the elevation of the sensor. Also, it is notable the presence of low frequencies only in the signal of the BE receiver (R).

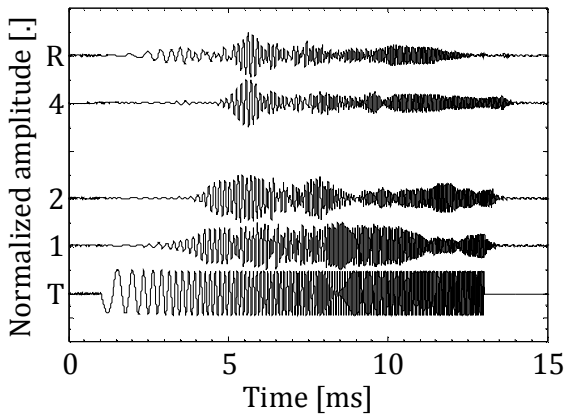

Figure 4. FD test (σ_0=50 kPa) Maximum amplitude: T[0.562V]; 1[1.478g]; 2[1.044g]; 4[1.487g]; R[0.055V]

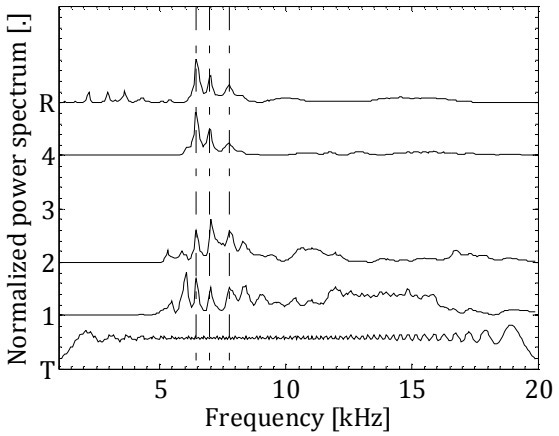

Figure 5. Normalized spectrum of a FD test (σ_0= 50 kPa)

4.3 RC tests

Table presents the results of the RC tests. Shear moduli G, were compared with Eq. 7 (Iwasaki and Tatsuoka, 1977) showing good agreement for all tests. For Toyoura sand and shear strain, $\gamma=10^{-5}$,A is equal to 11.085 and m is equal to 0.44.

$$G=A\frac{(2.17-e)^2}{1+e}\sigma_0{}^m \qquad [9]$$

Table 1.Results of RC tests

σ_0 [kPa]	γ	ξ [%]	V_S [m/s]	G [MPa]
50	1.2×10^{-5}	0.85	213	69.3
100	1.1×10^{-5}	0.72	261	103.9
200	9.1×10^{-6}	0.69	309	145.2
400	7.4×10^{-6}	0.67	351	187.4

5 ANALYSIS OF EXPERIMENTAL RESULTS

5.1 TD tests

Shear wave velocities for all confining pressures were obtained by recording data similar to that presented in Figure 3. The shear wave velocity was computed between different sensors: T-R, T-4, 1-4 and 1-R.

Figure 6 presents a comparison between these velocities and that obtained by the RC test. Dotted line represents the average of TD tests. The group of tests allows observing the following general behaviour:

The arrival time measured in the Acc. 2 is lower than the expected arrival timed computed by average velocity. This fact can be verified for all confinements. In addition, the amplitude increases with confinement, which is contrary to measurements seen in Acc. 4 and R. Acc. 2 could be influenced by other type of waves, for example compression waves originated by the lobes of T and reflected in the lateral boundary.

The maximum amplitude of the vibration measured by Acc. 1 remains more or less constant with confinement. The short distance from the source and the consequent small geometric attenuation could be the cause. It means that the amplitude of the perturbation is nearly constant despite the differences of the material stiffness.

The amplitude of the response measured in R and Acc. 4 decreases with the confinement. The higher stiffness of the material reduces the vibration amplitude in these points.

Average shear wave velocities obtained by TD tests are too similar with those obtained by RC tests. The error varies from 1.8% to 4.7% being always the shear wave velocity estimated by TD tests lower than the value obtained by RC tests.

Accelerometer readings confirm the validity of the BE testing in time domain and the interpretation based on the first direct arrival. Apparently, the presence of the accelerometers did not produce an undesirable effect on the performance of the technique, taking into account the small difference between TD and RC results.

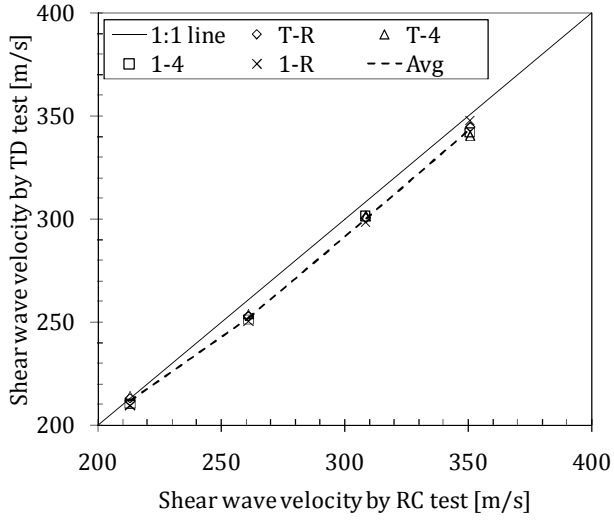

Figure 6. Comparison of results between TD and RC tests

5.2 FD tests

FD tests were done for all confining pressures recording time charts similar to that presented in Figure 4. Data was used to compute spectral densities and transfer functions by means of Eq. 5. Particular attention was paid to the shape of the transfer functions between T and R, H_{TR} that share similarities despite the different the soil stiffness.
Figure 7 shows a comparison of $|H_{TR}|$. Vertical and horizontal axes were normalized with respect to the magnitude of the highest peak and the frequency where the highest peak appears, respectively. Seven main peaks can be identified in the figure. Table 2 lists the specific frequencies of peaks indicated in Figure 7.

Peaks 1 to 4 correspond to the low frequencies that only appear in R as was pointed out in Figure 5. The proximity of this sensor with respect to the aluminum top cap and the high impedance of this border, allows to suggest that these low frequencies correspond to waves reflected against top and cap boundaries.

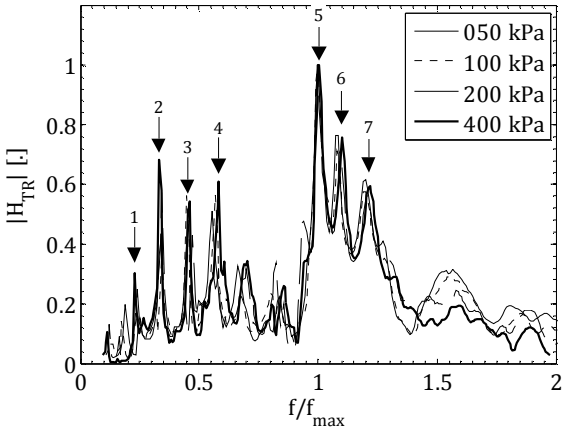

Figure 7. Comparison of normalized $|H_{TR}|$ in FD tests

These reflections of the waves against the end plates let an estimation of the shear wave velocity by using two consecutive frequency points, for example f_2 and f_3:

$$V_s=2L(f_3-f_2) \quad [10]$$

Where L is the total length of the specimen. The estimation of V_S by mean of Eq. 10 is included in Table 2.The limitation of this approach deals with the frequency resolution, which was 61 Hz for tests presented in this paper. This resolution in frequency produces a deviation of ±17 m/s in the estimation of the shear wave velocity. An increase of the sampling period to 1 second could improve the frequency resolution to 1 Hz.

Peaks 5 could represent the resonant frequencies of the BE Receiver inside the specimen. Given the soil and BE properties (ρ_s=1520 kg/cm^2,ν=0.3, E=6.2x10^{10} N/m^2,ρ=7500 kg/m^3, b=10 mm, h=0.6 and L=5 mm), Eq. 8 was used considering V_S listed in Table 1 and f_p#5 in Table 2. Thus, α=1.4566 and β=1.2958.

Table 2. Main frequency peaks in $|H_{TR}|$ and V_S by multiple reflections

σ_0 [kPa]	Frequency peaks, f_p [kHz] 1	2	3	4	5	V_S [m/s]
50		2.19	2.93	3.60	6.47	203
100		2.62	3.42	4.33	7.63	219
200	2.14	3.05	4.21	5.07	8.91	321
400	2.32	3.35	4.64	5.86	10.07	354

The estimation of the travel time t_t follows the procedure suggested by Viana da Fonseca *et al.*(2009): the travel time is computed by linear regression for different window bandwidths in the frequency range of the input signal. Figure 8 shows the results of this procedure. The circles indicate the central frequency were the correlation coefficient reaches the maximum value.

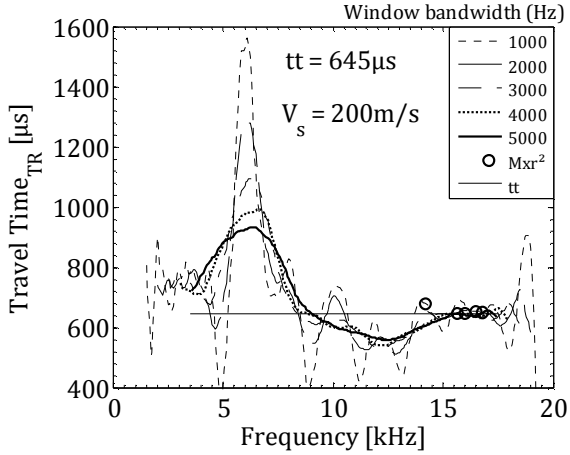

Figure 8. Estimation of the t_t in FD tests (σ_0=50 kPa)

Figure 9 presents the estimation of V_S compared against the value obtained by the RC tests. The dispersion is evident, especially as the soil stiffness increases.

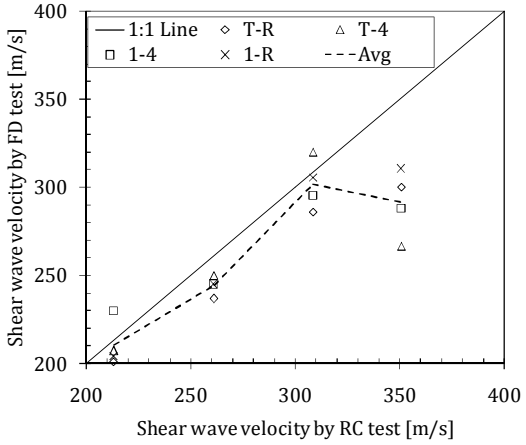

Figure 9. Comparison of results between FD and RC tests

6 SIMPLIFIED NUMERICAL SIMULATIONS

A simplified numerical simulation of a FD test is presented in this section. The simulation is done in order to understand the performance of the test and especially the procedure presented in Figure 8. The simulation does not try to reproduce the exact result but to use two simple models to approximate to a test. The analysis is based on the premise that the system can be decomposed in two parts: the subsystem (X-A) from the BE Transmitter (X) to Acc.1 (A); and the subsystem (A-R) from Acc. 1 to the BE Receiver. The model considers a soil specimen like the one presented previously. The shear wave velocity is equal to 213 m/s. The tip-to-tip distance is 128.3mm and the accelerometer is located 8.6 mm in front of BE transmitter.

The transfer function between sensors can be represented as a multi degree of freedom system (m-DOF), which is used to generate a simplified transfer function. Each mode m, is characterized by its own resonant frequency fr, dimensionless mass M, damping ratio ξ and phase Θ that were selected arbitrarily. The transfer function H(f) of this system is then computed by

$$H(f)=\sum_{m}\left\{\frac{\frac{e^{-i\Theta_m}}{(2\pi\cdot fr_m)^2\cdot M_m}}{1-\left(\frac{f}{fr_m}\right)^2-2\cdot i\cdot\xi_m\left(\frac{f}{fr_m}\right)}\right\} \qquad [11]$$

In addition, it is included a time shift due to the distance between sensors. The total transfer function $H_{XR}(f)$ is composed by two transfer functions in series: $H_{XA}(f)$ and $H_{AR}(f)$. The following two examples illustrate the effect of the peaks in the estimation of the travel time.

Model 1 represents a simple transfer function that does not have peaks above to 10 kHz (Figure 10a). Note that in the region where peaks appear, the dispersion of the estimated travel time is high and the average value is different than the theoretical value t_{XR} (Figure 10b). On the other hand, the region where no peaks are present, the best correlation coefficients take place and the estimation match with the actual value.

Model 2 includes a complex transfer function. The region above to 10kHz, even containing small peaks (Figure 11a), they produce undesirable effects in the estimation of the travel time, as can be seen in Figure 11b, in which the location of the points with the best correlation coefficients does not predict the correct value, t_{XR}.

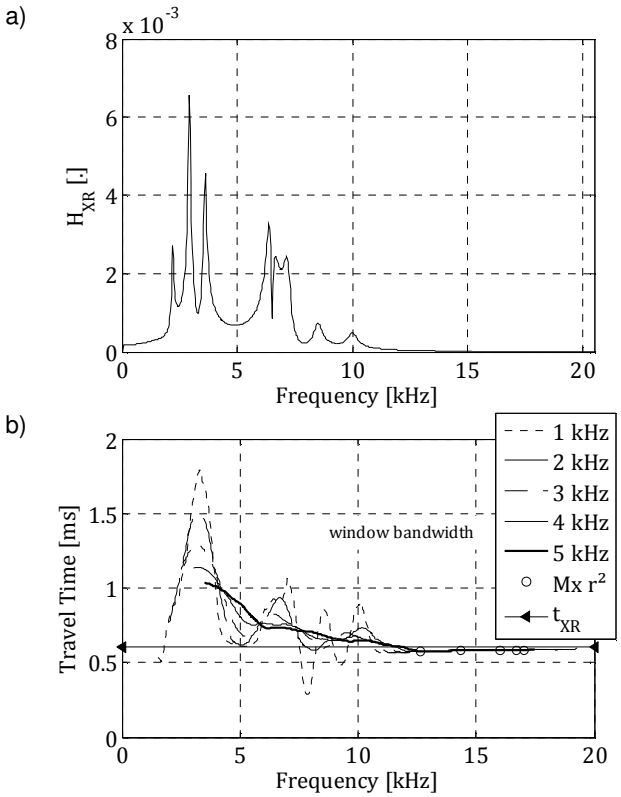

Figure 10.Model 1: a) $H_{XR}(f)$; b) estimation of t_t

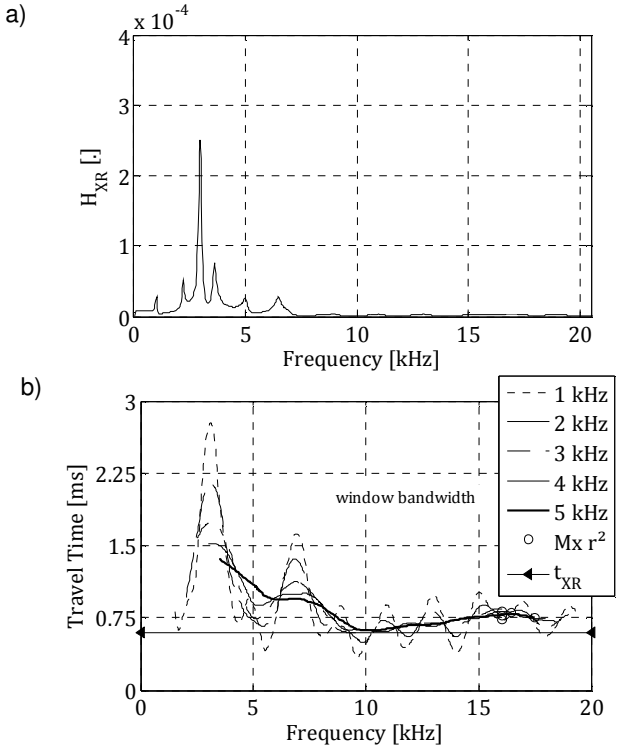

Figure 11.Model 2: a) $H_{XR}(f)$; b) estimation of t_t

CONCLUSIONS

An arrangement of miniature accelerometers was used to verify the performance of a BE system.

TD tests produced results in good agreement with the RC test. The first arrival time method was the one used for interpretation. The appropriate selection of the frequency of the sine pulse prevented the appearance of near-field effects.

The shear wave velocity computed between different combination of BE and accelerometers was approximately equal. The small standard deviation between these measurements suggests that the tip-to-tip distance is the correct travel distance.

Accelerometer 2 located near BE Transmitter shown an early arrival in comparison to the expected value, possibly caused by compressional waves generated by the lobes of the BE transmitter and reflected by the lateral boundaries. Accelerometers located at a greater distance do not have this problem because the compressional waves have small energy and attenuate faster.

Moreover experimental results and simplified numerical simulations allowed to understand the main causes of discrepancies of the frequency domain method.

Measurements show that the transfer function between BE transmitter and BE receiver has several peaks. These peaks are due to: (i) resonant frequencies of the BE, (ii) mode vibrations of the soil specimen, and (iii) wave reflections against ends. As the soil stiffness increases, the transfer function gradually changes, being the main characteristic of this change, the migration of the peaks to higher frequencies.

The travel time estimation should be done in a frequency range where no peaks appear. This ideal condition is not possible in actual testing. In consequence, an approximate estimation could be obtained if the frequency range is located as far as possible to the main peaks.

The shear wave velocity estimation by multiple reflections in frequency domain is a promissory alternative that could be performed in simultaneous with the FD test.

REFERENCES

Arroyo, M.; Muir Wood, D. and Greening, P. D. (2003). "Source near-Field Effects and Pulse Tests in Soils Samples" *Géotechnique*, 53(3), 337-345.

Arroyo, M.; Muir Wood, D.; Greening, P. D.; Medina, L. and Rio, J. (2006). "Effects of Sample Size on Bender-Based Axial G_0 Measurements" *Géotechnique*, 56(1), 39-52.

Arulnathan, R.; Boulanger, R. W. and Riemer, M. F. (1998). "Analysis of Bender Element Tests" *Geotechnical Testing Journal, ASTM*, 21(2), 120-131.

ASTM International. (2002). "Standard Test Methods for Modulus and Damping of Soils by the Resonant-Column Method (D 4015-92)" Annual Book of Astm Standards, West Conshohocken.

Brignoli, E. G.; Gotti, M. and Stokoe, K. H. I. (1996). "Measurement of Shear Waves in Laboratory Specimens by Means of Piezoelectric Transducers" *Geotechnical Testing Journal, ASTM*, 19(4), 384-397.

Camacho-Tauta, J.; Santos, J. A.; Ferreira, C. and Viana da Fonseca, A. (2008). "Moving Windows Algorithm to Reduce Uncertainties in Bender Element Testing" *XI Portuguese National Congress of Geotechnics*, Portugese Society of Geotechnics, Coimbra, 149-156.

Cascante, G.; Vanderkooy, J. and Chung, W. (2005). "A New Mathematical Model for Resonant-Column Measurements Including Eddy-Current Effects" *Canadian Geotechnical Journal*, 43(4), 121-135.

Dyvik, R. and Madshus, C. (1985). "Lab Measurements of G_{max} Using Bender Elements" *Proc., ASCE Annual Convention on Advances in the Art of Testing Soils under Cyclic Conditions*, Khosla, V., ed., Detroit, Michigan, 186-196.

Ferreira, C.; Martins, J. P. and Gomes Correia, A. (2010). "Implementation of Bender-Extender Elements and Accelerometers in a Stress-Path Triaxial Cell" *12th Portuguese National Congress of Geotechnics*, Gomes Correia, A., ed., Universidade do Minho, Guimarães, 247-256 (in Portuguese).

Ferreira, C.; Viana da Fonseca, A. and Santos, J. A. (2006). "Comparison of Simultaneous Bender Element Test and Resonant Column Tests on Porto Residual Soils" Soil Stress-Strain Behavior: Measurement, Modeling and Analysis. A Collection of Papers of the Geotechnical Symposium in Rome, March 16–17, 2006, Ling, H. I.; Callisto, L.; Leshchinsky, D. and Koseki, J., eds., Springer, 523-536.

Greening, P. D. and Nash, D., F.T. (2004). "Frequency Domain Determination of G_0 Using Bender Elements" *Geotechnical Testing Journal, ASTM*, 27(3), 1-7.

Ismail, M.; Sharma, S. S. and Fahey, M. (2005). "A Small True Triaxial Apparatus with Wave Velocity Measurement" *Geotechnical Testing Journal, ASTM*, 28(2), 113-122.

Iwasaki, T. and Tatsuoka, F. (1977). "Effects of Grain Size and Grading on Dynamic Shear Moduli of Sands" *Soils and Foundations*, 17(3), 19-35.

Jovičić, V.; Coop, M. R. and Simić, M. (1996). "Objetive Criteria for Determining G_{max} from Bender Element Tests" *Géotechnique*, 46(2), 357-362.

Kaarsberg, E. A. (1975). "Elasic-Wave Velocity Measurements in Rocks and Other Materials by Phase-Delay Methods" *Geophysics*, 40(6), 955-960.

Lee, J.-S. and Santamarina, J. C. (2005). "Bender Elements: Performance and Signal Interpretation" *Journal of Geotechnical and Geoenvironmental Engineering, ASCE*, 131(9), 1063-1070.

Maqbol, S. and Koseki, J. (2008). "Development of an S-Wave Measurement System for Laboratory Specimens" *Deformational Characteristics of Geomaterials*, Burns, S. E.; Mayne, P. W. and Santamarina, J. C., eds., IOS Press, Atlanta, GA, 711-715.

Nishio, S. and Tamaoki, K. (1988). "Measurement of Shear Wave Velocities in Diluvial Samples under Triaxial Conditions" *Soils and Foundations*, 28(2), 35-48.

Pallara, O.; Mattone, M. and Lo Presti, D. C. F. (2008). "Bender Elements: Bad Source - Good Receiver" *Deformational Characteristics of Geomaterials*, IOS Press, Atlanta, 697-702.

Rio, J. (2006). "Advances in Laboratory Geophysics Using Bender Elements", PhD Thesis, University of London, London.

Rio, J.; Greening, P. and Medina, L. (2003). "Influence of Sample Geometry on Shear Wave Propagation Using Bender Elements" *Deformation Characteristics of Geomaterials*, Swets and Zeitlinger., B. V., eds., Balkema, Lyon, 963-967.

Sanchez-Salinero, I.; Roesset, J. M. and Stokoe, K. H. I. (1986). "Analytical Studies of Body Wave Propagation and Attenuation", Report GR 86-15, University of Texas, Austin.

Santos, J. A.; Camacho-Tauta, J.; Parodi, M.; Viana da Fonseca, A. and Ferreira, C. (2007). "Use of Random Vibrations to Measure Stiffness of Soils" *Experimental Vibration Analysis for Civil Engineering Structures (EVACES'07)*, Cunha, A. and Caetano, E., eds., University of Porto, Porto, 1169-1178.

Shirley, D. J. (1978). "An Improved Shear Wave Transducer" *J. Acoust. Soc. Am.*, 63(5), 1643-1645.

Shirley, D. J. and Hampton, L. D. (1978). "Shear-Wave Measurement in Laboratory Sediments" *J. Acoust. Soc. Am.*, 63(2), 607-613.

Viana da Fonseca, A.; Ferreira, C. and Fahey, M. (2009). "A Framework Interpreting Bender Element Tests, Combining Time-Domain and Frequency-Domain Methods" *Geotechnical Testing Journal, ASTM*, 32(2), 1-17.

Viggiani, G. and Atkinson, J. H. (1995). "Interpretation of Bender Element Tests" *Géotechnique*, 45(1), 149-154.

Wicaksono, R. I.; Tsutsumi, Y.; Sato, T.; Koseki, J. and Kuwano, R. (2008). "Stiffness Measurements by Cyclic Loading, Triggger Accelerometer, and Bender Element on Sand & Gravel" *Deformational Characteristics of Geomaterials*, Burns; Mayne and Santamarina, J. C., eds., IOS Press, Atlanta, GA, 733-739.

Yamashita, S.; Kawaguchi, T.; Nakata, Y.; Mikami, T.; Fujiwara, T. and Shibuya, S. (2009). "Interpretation of International Parallel Test on Measurement of G_{max} Using Bender Elemens" *Soils and Foundations*, 49(4), 631-650.